

Phase transitions in nanosystems caused by interface motion: The Ising bipyramid with competing surface fields

A. Milchev,^{1,2} M. Müller,^{1,3} and K. Binder¹¹*Institut für Physik, WA 331, Johannes Gutenberg Universität, D 55099 Mainz, Germany*²*Institute for Physical Chemistry, Bulgarian Academy of Sciences, 1113 Sofia, Bulgaria*³*Department of Physics, University of Wisconsin-Madison, 1150 University Avenue, Madison, Wisconsin, 53706-1390, USA*

(Received 10 May 2005; revised manuscript received 29 July 2005; published 16 September 2005)

The phase behavior of a large but finite Ising ferromagnet in the presence of competing surface magnetic fields $\pm H_s$ is studied by Monte Carlo simulations and by phenomenological theory. Specifically, the geometry of a double pyramid of height $2L$ is considered, such that the surface field is positive on the four upper triangular surfaces of the bipyramid and negative on the lower ones. It is shown that the total spontaneous magnetization vanishes (for $L \rightarrow \infty$) at the temperature $T_f(H)$, related to the “filling transition” of a semi-infinite pyramid, which can be well below the critical temperature of the bulk. The discontinuous vanishing of the magnetization is accompanied by a susceptibility that diverges with a Curie-Weiss power law, when the transition is approached from either side. A Landau theory with size-dependent critical amplitudes is proposed to explain these observations, and confirmed by finite size scaling analysis of the simulation results. The extension of these results to other nanosystems (gas-liquid systems, binary mixtures, etc.) is briefly discussed.

DOI: [10.1103/PhysRevE.72.031603](https://doi.org/10.1103/PhysRevE.72.031603)

PACS number(s): 68.08.Bc, 05.70.Fh, 68.35.Rh, 64.60.Fr

I. INTRODUCTION

The current paradigm of attempting to develop various kinds of nanoscopic devices requires careful consideration of the phase behavior of nanosystems, since in nanoscopic geometries effects due to external walls or other boundaries of the system can modify its “bulk” behavior substantially. Qualitatively new kinds of phenomena may occur that have not yet been studied for macroscopic bulk systems.

We demonstrate another kind of phase transition in the present paper, which belongs to the class of interface localization-delocalization phenomena, using the simple Ising ferromagnet with nearest-neighbor exchange on a cubic lattice as a generic example. Choosing a compact octahedral shape of the system in the form of a bipyramid of height $2L$, we assume that on the upper surfaces of the pyramid ($0 < z \leq L$) a positive surface magnetic field $+H_s$ acts, while on the lower surfaces (with $-L \leq z < 0$) the field is negative but of the same absolute strength, so that no sign of the magnetization is overall preferred. More generally, one might consider the case with positive and negative fields of different strength; their difference, however, could be effectively compensated by a suitably chosen bulk field such that at low temperatures again a degeneracy with respect to the sign of the spontaneous magnetization is possible, similar to the case of “capillary condensation”-type phenomena in semi-infinite thin films [1–11]. In this case one can also expect an interesting interplay between the wetting behavior of the semi-infinite system and the phase behavior in confinement, a complication that is not considered in the present manuscript.

Such a system is then described (for $L \rightarrow \infty$) by an order parameter (the spontaneous magnetization of the Ising ferromagnet), which does *not* remain non zero up to the critical temperature T_{cb} of the bulk three-dimensional model, but rather only up to a temperature $T_f(H_s)$, identical with the

(critical) temperature of the filling transition [12–30] in a single semi-infinite pyramid. As will be discussed in this paper, this kind of phase transition [31] in the limit $L \rightarrow \infty$ can be either of first order or of second order, depending on the value of the line tension, which describes [32–37] the free energy excess associated with the contact line where the interface separating oppositely oriented domains meets the free surface (or inert wall that confines the system, respectively). Of course, as long as the linear dimension L of the system is large but finite, finite-size rounding of this phase transition needs to be considered, and hence we shall present a tentative generalization of the theory of finite size scaling [38–45] to the present situation.

A qualitative explanation of this transition is sketched in Fig. 1. It is assumed that the surface magnetic field strength H_s is small enough, so that for zero temperature the ground state of the system has a uniform (positive or negative) magnetization, in spite of the unfavorable energy cost due to the surfaces (or walls, respectively) where the surface magnetic field is oppositely oriented to the direction of the spontaneous magnetization. As the temperature is raised, the interfacial free energy σ between oppositely oriented domains decreases faster than the excess free energy difference, $f_s(H_s, T)$, of a positively oriented domain between surfaces with $\pm H_s$. As is well known the interfacial free energy σ vanishes at the bulk critical temperature T_{cb} according to a power law $\sigma \propto (1 - T/T_{cb})^{2\nu_b}$ with the correlation length critical exponent [46,47] $\nu_b \approx 0.63$. At the temperature $T_f(H_s)$, these surface free energies become equal, and hence for $T > T_f(H_s)$ it is energetically favorable to have a state with two oppositely magnetized domains, separated by an interface located in the basal plane of the bipyramid (Fig. 1). Of course, in the actual calculation of $T_f(H_s)$ not only the surface free energies σ and $f_s(H_s, T)$ (per unit area) matter, but one must also consider the fact that the four triangular surfaces take a larger area (depending on the opening angle α of

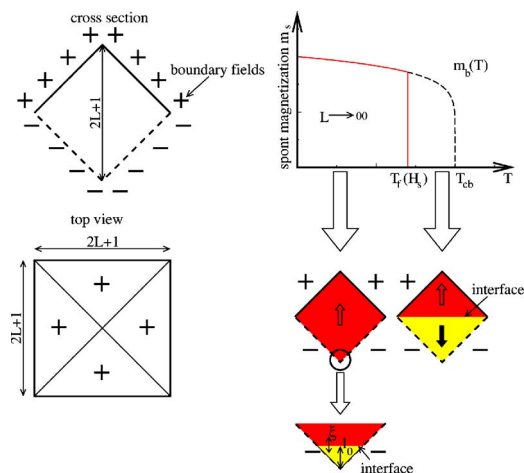


FIG. 1. (Color online) Ising ferromagnet on a simple cubic lattice whose surfaces form a bipyramid (left) and resulting phase transition in the limit $L \rightarrow \infty$ (right), plotting the spontaneous magnetization $m_s(T)$ versus temperature T . Signs (+, -) along the cross section of the bipyramid (left upper part) or on the triangular projections of the surfaces in the top view (left lower part) refer to the surface magnetic field, $\pm H_s$, that acts on the spins in the surface planes only. Note that the basal plane of the bipyramid is taken to be the (xy) plane of the simple cubic lattice, and measuring lengths in units of the lattice spacing, each pyramid takes L planes (with a single spin in the pyramid top), so the total linear dimension from top to bottom of the bipyramid is $2L+1$ (the extra lattice slice accounts for the basal plane common to both pyramids). For $T < T_f(H_s)$, the interface between the domains with negative (\downarrow) and positive (\uparrow) magnetization is located close to one of the corners (e.g., the bottom corner, as assumed in the figure; see the magnified view). The local fluctuations of the interface extend over a correlation range ξ_{\perp} , as indicated by the double arrow. As the temperature is increased towards the filling transition temperatures, $T \rightarrow T_f(H_s)$, the interface detaches from the corner and moves towards the mid-plane of the bipyramid. For $T > T_f(H_s)$ the magnetization m_s then remains zero.

the pyramids) than the area of the interface. In this work, we consider explicitly only the case $\alpha=45^\circ$, so that the surfaces of the bipyramid meet at the basal plane at an angle of 90° , but it is clear that the general features of the phenomena described here do not depend on this particular choice. In fact, we speculate that also the choice of planar surfaces is an irrelevant detail, and similar behavior could be observed for other geometries such as double cones with different surface fields on the upper and lower portion.

The outline of this paper is as follows. In Sec. II, we recall the basic facts about the filling transition in semi-infinite cones, and develop a tentative phenomenological theory for describing the transition explained in Fig. 1. Section III describes our Monte Carlo results and interprets them in terms of the phenomenological description of Sec. II. Finally Sec. IV contains our conclusions, and discusses briefly the extension to phase transitions of other systems (gas-liquid systems, binary mixtures, etc.) in related geometries.

II. THEORETICAL BACKGROUND

In this section two complementary phenomenological approaches to the phase transition in a double pyramid are de-

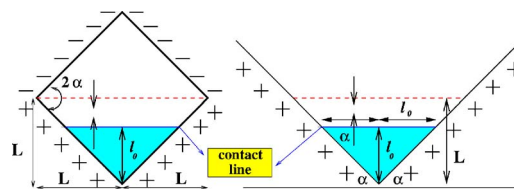


FIG. 2. (Color online) Comparison of a bipyramid of height $2L$ and basal plane of linear dimension $2L$ with a single (infinitely large) pyramid, assuming the same positive surface field H_s at the corresponding surfaces, and considering the situation that the interface between the domains with positive (\uparrow) and negative (\downarrow) magnetization is located at the same distance ℓ_0 from the bottom corner in both cases. An opening angle $\alpha=45^\circ$ is assumed for simplicity.

veloped. In subsection A we use the description of the filling of a single cone [21]. This yields the location of the filling transition in the limit $L \rightarrow \infty$ and we discuss modifications due to the double-pyramid geometry. This approach is expected to yield a good description if the magnetization is close to its saturation value, i.e., for $Lt \gg 1$, where t denotes the reduced distance from the filling transition. The role of fluctuations within this context is considered in subsection B. Then, in subsection C, we develop a phenomenological Landau-type theory for the case that the interface fluctuates around the basal plane. This approach is able to describe the behavior in the ultimate vicinity of the transition, $L^2 t \ll 1$, and the fluctuations above the transition.

A. Phenomenological considerations in terms of surface thermodynamics

Our phenomenological description assumes that the theory of cone filling [21] can be directly applied to the filling of a semi-infinite pyramid (i.e., we ignore the excess free energy at the edges of the pyramid, where the contact lines of the interface with two triangular pyramid surfaces meet). We compare the bipyramid geometry to an equivalent situation of a semi-infinite single pyramid, and consider the case when the interface is located at a height ℓ_0 above the bottom corner (Fig. 2). We write the free energy of the semi-infinite pyramid, relative to a state with no interface, in terms of surface and line free energies

$$\Delta F_s = 4\ell_0^2 \sigma + 8\ell_0 \sigma_{\text{line}} - 4\sqrt{2}\ell_0^2 f_s(H_s). \quad (1)$$

In Eq. (1), we have used the geometrical factors appropriate for the opening angle $\alpha=45^\circ$ (a generalization in terms of other choices for the angle α is straightforward), and we have also suppressed temperature arguments throughout, in order to simplify the notation. Actually, rather than using the temperature, T , as a control parameter as assumed in Fig. 1, we find it more convenient to use the strength of the surface magnetic field H_s instead. [In the plane of variables T, H_s the filling transition line is described by the inverse function $H_{sc}(T)$ of the function $T_f(H_s)$. As long as one crosses this line under a finite angle, it does not matter whether T or H_s is used as a control variable].

Since we know that at the filling transition the interface can move infinitely far apart from the lower corner, $\ell_0 \rightarrow \infty$, we must have $\Delta F=0$ for $H_s=H_{sc}$, i.e.,

$$\sigma = \sqrt{2}f_s(H_{sc}). \quad (2)$$

This result agrees with the macroscopic filling condition that the cone fills if the contact angle on a planar substrate equals the cone angle, α . In the vicinity of H_{sc} the variation of $f_s(H_s)$ with H_s is linear, $f_s(H_s) = f_s(H_{sc}) + (H_s - H_{sc})f'_s$. As a result, near $H_s = H_{sc}$ Eq. (1) can be rewritten as

$$\Delta F_s(\ell_0) = 8\ell_0\sigma_{\text{line}} - 4\sqrt{2}\ell_0^2(H_s - H_{sc})f'_s. \quad (3)$$

Minimization of Eq. (3) with respect to ℓ_0 readily yields

$$\ell_0 = \frac{\sigma_{\text{line}}}{\sqrt{2}(H_s - H_{sc})f'_s}. \quad (4)$$

Since $f_s(H_s)$ is a monotonously increasing function of H_s , $f'_s > 0$ and hence the denominator of Eq. (4) is *negative* in the considered region $H_s < H_{sc}$ (for $H_s > H_{sc}$ the pyramid is “filled,” i.e., $\ell_0 \equiv \infty$ on this other side of the filling transition). Of course, only non-negative solutions for ℓ_0 are physically meaningful, and hence we require that the line tension is negative, $\sigma_{\text{line}} < 0$. The fact that critical cone filling can only occur for negative values of the line tension has already been stressed by Parry *et al.* [21]. If $\sigma_{\text{line}} \geq 0$, only a first order filling transition is possible (i.e., at $H_s = H_{sc}$ the length ℓ_0 jumps discontinuously from $\ell_0 = 0$ to $\ell_0 = \infty$ in our simplified treatment). Using Eq. (4) in Eq. (3) yields

$$\Delta F_s = 2\sqrt{2}\sigma_{\text{line}}^2 \frac{1}{(H_s - H_{sc})f'_s}. \quad (5)$$

One should not worry about the fact that for $H_s \rightarrow H_{sc}$ this free energy excess $\Delta F_s \rightarrow -\infty$, because ΔF in Eqs. (3) and (5) is of order unity only, rather than scaling with any power of the linear dimension of the system. For the filling transition, the relevant free energy scale is $4\sigma L^2$, if for $H_s < H_{sc}$ we have an interface of area $(2L)^2$ in the system. The free energy depression per unit area resulting from Eq. (5) is of order $[(H_s - H_{sc})L^2]^{-1}$ and, hence, for $|H_s - H_{sc}|$ of order L^{-2} the divergence in Eq. (5) becomes problematic. Taking the limit $L \rightarrow \infty$ first, and then letting $H_s \rightarrow H_{sc}$ obviously poses no problem: the free energy per unit area stays $4\sqrt{2}f_s(H_s, T)$ for $H_s < H_{sc}$.

We suggest now that in a large but finite bipyramid the behavior of the surface free energies gets modified as schematically shown in Fig. 3. For $H > H_{sc}(L)$ the interface is located at $\ell_0 = L$, in the basal plane of the bi-pyramid, and the free energy is reduced by a line tension contribution, $f = 4\sigma L^2 + 8\sigma'_{\text{line}}L$. Note that, in general, the line tension of an interface in the basal plane of the bi-pyramid, σ'_{line} , where two planes (with surface fields $+H_s$ and $-H_s$) meet under an angle 2α (Fig. 2, left part), can be expected to differ from the line tension σ_{line} of an interface that meets a flat surface under an angle α (Fig. 2, right part), with a surface field $+H_s$ on both sides of the interface. It is the latter quantity, however, which determines the scale of the depression ΔF_s below the leading variation $4\sqrt{2}L^2f_s(H_s) = 4\sigma L^2 + 4\sqrt{2}L^2f'_s(H_s - H_{sc})$. Since properties like the total magnetization of the bipyramid change continuously, when ℓ_0 increases from small values to $\ell_0 = L$, it is assumed that the transition from the state with broken symmetry (the interface being located

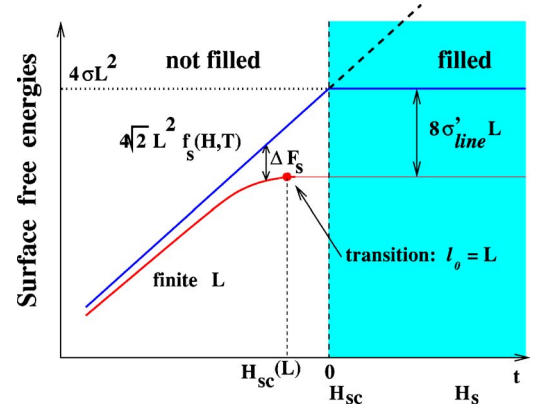


FIG. 3. (Color online) Schematic plot of the surface free energies of a large but finite bipyramid Ising system versus H_s (or $t = H_s/H_{sc} - 1$, respectively). For $L \rightarrow \infty$ the surface free energy is $4\sqrt{2}L^2f_s(H, T)$ for $H_s < H_{sc}$, since the contribution due to the interface at height ℓ_0 above the lower corner is negligible. For H_s near H_{sc} the variation of $f_s(H, T)$ with H_s is linear. For $H_s > H_{sc}$ the surface free energy is due to the interface in the basal plane of the bipyramid, $4\sigma L^2$, independent of H_s , in the limit $L \rightarrow \infty$. If large but finite linear dimensions L are considered, the surface free energies are reduced because of line tension contributions. For $H_s > H_{sc}(L)$, which is characterized by $\ell_0 = L$ (dot in the figure), this reduction is $8\sigma'_{\text{line}}L$ (in the vicinity of H_{sc} the dependence of σ'_{line} on H_s can be neglected). For $H_s < H_{sc}(L)$, the depression ΔF_s of the surface free energy relative to its asymptotic expression for $L \rightarrow \infty$ gradually grows with increasing H_s , reflecting the gradual increase of ℓ_0 . Assuming that the gradual motion of $\ell_0 \rightarrow L$ can be described analogous to a second-order transition in a bulk system, the free energy is drawn to meet the branch $4\sigma L^2 - 8\sigma'_{\text{line}}L$ at $H_{sc}(L)$ with horizontal slope.

at ℓ_0 or $2L - \ell_0$, respectively) for $H_s < H_{sc}(L)$ to the symmetric state where $\ell_0 = L$ is a *second order* transition, implying that the two branches of the surface free energy meet at $H_s = H_{sc}(L)$ with a common tangent. In our notation (and in Fig. 2) we have allowed for a shift of $H_{sc}(L)$ due to finite size from its asymptotic value $H_{sc} \equiv \lim_{L \rightarrow \infty} H_{sc}(L)$. Of course, in reality we must expect that for finite L there is a rounding of the transition in addition to the shift, and hence there does not exist any value $H_{sc}(L)$ where singularities of the considered model (Figs. 1 and 2) occur for finite L , but this rounding of the transition can only be allowed for if statistical fluctuations are taken into account.

If one could take the result for the free energy depression through the formation of an interface, Eq. (5), literally, the resulting behavior of the surface free energies would even be slightly more complicated than conjectured in Fig. 3. In fact, if we consider the surface free energy for $H_s < H_{sc}(L)$ explicitly

$$f(H_s) = 4\sigma L^2 + 4\sqrt{2}L^2(H_s - H_{sc})f'_s + \Delta F_s, H_s < H_{sc}(L) \quad (6)$$

and insert Eq. (5), we recognize that $f(H_s)$ exhibits a maximum at

$$H_s(L)_{max} - H_{sc} = \frac{\sigma_{line}}{\sqrt{2f'_s}L}, \quad (7)$$

which corresponds to a value $\ell_0=L$. Using this result in Eq. (6), we readily find $f(H_s)=4\sigma L^2+8\sigma_{line}L$ at the point marked by a dot in Fig. 3, as $H_s \rightarrow H_{sc}^-(L)$. On the other hand, approaching the transition from the other side [$H_s \rightarrow H_{sc}^+(L)$], we have $f(H_s)=4\sigma L^2+8\sigma'_{line}L$, and there is *a priori* no reason to assume that $\sigma_{line}=\sigma'_{line}$ as noted above, because of the physical distinction between the contact line on a plane and the contact line pinned to the edge where the surface field changes sign (cf. Fig. 2). So one would predict that in the surface free energy at $H_{sc}(L)$ there is a jump singularity of order L . However, as will be discussed in the next section, thermal fluctuations are expected to smooth out this singularity and, hence, $f_s(H_s)$ is a smooth nonsingular function for all L .

B. Interfacial fluctuations at filling transitions

Here we recall results due to Parry *et al.* [21] on the filling of rotationally symmetric (infinite) cones. These authors presented arguments that the dominating fluctuations of the interface are the so-called “breather modes,” i.e., the interface moves *uniformly* up or down. If we denote this fluctuating height of the interface midpoint over the cone (or pyramid) corner as ℓ and interpret ℓ_0 of the previous subsection as its average value, $\ell_0=\langle\ell\rangle$, the probability distribution derived by Parry *et al.* [21] for the interface position ℓ can be rewritten as

$$P(\ell) \propto \exp\left[-\frac{1}{2\xi_{\perp}^2}(\ell - \ell_0)^2\right], \quad (8)$$

where the correlation length ξ_{\perp} describing the interfacial width due to these breather fluctuations diverges by a simple power law

$$\xi_{\perp} \propto |t|^{-\nu_{\perp}}, \quad \nu_{\perp} = \frac{1}{2}. \quad (9)$$

Although Eqs. (8) and (9) have been directly obtained for axially symmetric cones only, Parry *et al.* [21] assert that they should hold as well for the inverted pyramid-shaped geometry considered in the right part of Fig. 2.

It is interesting to apply Eqs. (8) and (9) to such a semi-infinite inverted pyramid for the case when ℓ_0 has reached the value $\ell_0=L$. Then Eqs. (8) and (9) imply, using $\ell_0 \propto t^{-1}$,

$$\langle\ell^2\rangle - \langle\ell\rangle^2 = \xi_{\perp}^2 \propto |t|^{-1} \propto \ell_0 \propto L. \quad (10)$$

This result also means, however, that the fluctuation in the area of the interface is proportional to L as well. Since these fluctuations of the interfacial free energy are of the same order as the contribution of the line tension, a theory based on balancing surface free energy differences with the line tension alone, as sketched in the previous subsection, cannot be expected to be quantitatively valid. Basically, one could argue, what needs to be done is to average the free energy function of the previous section with the Gaussian distribution resulting from Eq. (8): the result will then be a renor-

malized effective free energy varying smoothly with H_s , as anticipated in Fig. 3.

Equation (10) yields a justification for the assumption that only the uniform “breather” mode needs to be taken into account while all the nonuniform interfacial fluctuations can be neglected. As is well known, long wavelength nonuniform interfacial fluctuations can be modeled as capillary waves [33,48–52] and over a length scale L these capillary waves cause a broadening of the interfacial profile described by the following expression for the mean square width w^2

$$w^2 = w_0^2 + \frac{k_B T}{4\sigma} \ln \frac{L}{B}, \quad (11)$$

where w_0 is a (hypothetical [53]) intrinsic width and B is a short wavelength cutoff of the same order as w_0 . The logarithmic variation of w^2 with L in Eq. (11) results from integrating the mean square amplitude $\langle|h(\vec{q})|^2\rangle$ of the Fourier components $h(\vec{q})$ of the deviation $h(\vec{x})=\ell(\vec{x})-\langle\ell\rangle$ of the local height of the interface $\ell(\vec{x})$ from its average value $\langle\ell\rangle$,

$$\langle|h(\vec{q})|^2\rangle = \frac{k_B T}{\sigma q^2} \quad (12)$$

over all wave numbers q in the interval $2\pi/L \leq q \leq 2\pi/B$.

The dominance of the uniform “breather mode” over the nonuniform capillary waves is not unique to the problem of the filling transition. Also in the problem of interface localization-delocalization transitions in thin films [5,54–59] of thickness D a related anomalous size dependence of interfacial widths was observed [60]. Specifically, it was found that for a fixed linear dimension L parallel to the competing walls (in the “soft mode” phase [54,55] where the interface is unbound from the walls) the mean square fluctuation of the interface scales even quadratically with D [60]

$$w^2 \propto \frac{k_B T \kappa D^2}{\sigma L}, \quad D \rightarrow \infty, L \text{ fixed}, \quad (13)$$

corresponding to a fluctuation of the interface as a whole in the direction normal to the interface over a finite fraction of the film thickness. In Eq. (13), κ^{-1} is a length characterizing the exponential decay of the (short range) repulsive effective potential acting on the interface from the wall at $z=0$, $V(z) \propto \exp[-\kappa z] + \exp[-\kappa(D-z)]$, z being the distance of the mean position of the interface from the left wall. In the opposite limit, a linear variation of the mean square fluctuation with D was found [60,61]

$$w^2 = w_0^2 + \frac{k_B T \kappa D}{16\sigma} + \text{const}, \quad L \rightarrow \infty, D \gg w_0. \quad (14)$$

For a cubic geometry $D=L$ we note that Eqs. (13) and (14) exhibit a smooth crossover characterized by

$$w^2 \propto \frac{k_B T}{\sigma} \kappa L, \quad L \rightarrow \infty, \quad (15)$$

which is the same type of relation as found above in the context of the filling transition, Eq. (10). Unfortunately, when the interface average position coincides with the bi-pyramid basal plane (Fig. 2, left part), the effective interface

potential is not known to us, and hence we cannot quantify the prefactor in the relation $w^2 = \langle \ell^2 \rangle - \langle \ell \rangle^2 \propto L$ in this case.

C. A phenomenological Landau-like theory for the phase transition of the Ising bipyramid

As discussed in the previous sections, the phase transition sketched in Fig. 1 cannot be understood solely from a macroscopic balance of surface and line free energies, but interfacial fluctuations must be taken into account, and the dominating fluctuation that needs to be considered, is a uniform fluctuation of the position ℓ of the interface around its average position ℓ_0 , in Fig. 2 (left part). However, to a first approximation, ℓ_0 is related to the total magnetization per spin, m , by

$$m/m_b = [1 - (\ell_0/L)^3], \quad (16)$$

where m_b is the bulk magnetization of an (infinite) Ising lattice at the same temperature. Here we use simple geometrical relations, noting that the volume of the total bipyramid is $8L^3/3$, the volume which has opposite orientation of the magnetization is $4\ell_0^3/3$, and we have neglected any surface contributions to the magnetization, assuming that the local magnetization is everywhere $\pm m_b$ in the bipyramid, right up to the surfaces and to the interface. We shall discuss corrections to this approximation below.

Being interested in $|m|/m_b \ll 1$, it makes sense to transform from ℓ_0 to $\tilde{\ell}_0 = L - \ell_0$, i.e., we count the interface distance from the basal plane rather than the lower pyramid corner, to conclude that in this limit $m/m_b \approx 3\tilde{\ell}_0/L$. Thus we conclude that $(\langle m \rangle - m)/m_b \approx 3(\ell_0 - \ell)/L$, and hence Eq. (8) can be rewritten as (in the following we take $m_b \equiv 1$ as the unit of the magnetization per spin)

$$P(m) \approx \exp\left[-\frac{L^2}{18\xi_{\perp}^2}(m - \langle m \rangle)^2\right]. \quad (17)$$

Remembering that $\xi_{\perp} \propto |t|^{-1/2}$ [Eq. (9)] this is equivalent to

$$P(m) \approx \exp[-\text{const}L^2(-t)(m - \langle m \rangle)^2]. \quad (18)$$

Comparing this expression with the general fluctuation formula [42,62]

$$P(m) \propto \exp\left[-\frac{V(m - \langle m \rangle)^2}{2k_B T \chi}\right], \quad (19)$$

$V = 8L^3/3$ being the volume of the system, we immediately conclude that the susceptibility per spin χ at the transition of Fig. 1 satisfies a Curie Weiss law for $t < 0$ (i.e., $H_s < H_{sc}$)

$$\chi \propto L/|t|. \quad (20)$$

Note that Eq. (20) holds only for $L^2|t| \gg 1$, because only then is Eq. (18) sharply peaked at $m \approx \langle m \rangle$, and the Gaussian approximation for $P(m)$ holds. It is also interesting to note that the ‘‘critical amplitude’’ [63] Γ_{-} in the power law $\chi = \Gamma_{-}|t|^{-\gamma}$ is proportional to L , i.e., divergent in the thermodynamic limit. However, this fact is trivially understood, since the bulk magnetic field creates a Zeeman energy $H\langle m \rangle(8L^3/3)$, scaling with volume, while shifting the interface between the

oppositely oriented domains costs an energy proportional to the interface area (of order L^2) only.

For $H_s > H_{sc}$ (i.e., $t > 0$) we expect that the susceptibility per spin, χ , in the analogous relation where $\langle m \rangle \equiv 0$,

$$P(m) \propto \exp\left[-\frac{1}{2}Vm^2/(k_B T \chi)\right], \quad (21)$$

also scales proportional to L , because the above argument with the Zeeman energy remains valid. Hence it is tempting to assume that there holds a Curie-Weiss law analogous to Eq. (20) also for $t > 0$, and we suggest therefore that

$$P(m) \propto \exp[-\text{const}L^2|t|m^2], \quad t > 0, L^2|t| \gg 1, \quad (22)$$

in analogy with Eq. (18). Now we also remember that for $t < 0$ there is a symmetry with respect to the sign of the magnetization, so Eq. (18) for $H=0$ really needs to be replaced by an expression that is symmetric with respect to the sign of $\langle m \rangle = \pm m_0$,

$$\begin{aligned} P(m) &\propto \frac{1}{2}\{\exp[-\text{const}L^2(-t)(m - m_0)^2] \\ &\quad + \exp[-\text{const}L^2(-t)(m + m_0)^2]\} \\ &\approx \frac{1}{2}\exp\left[-\text{const}L^2(-t)\frac{(m - m_0)^2(m + m_0)^2}{4m_0^2}\right] \\ &\quad \text{for } |m| \approx m_0 \text{ and } L^2|t| \gg 1. \end{aligned} \quad (23)$$

It then is tempting to interpret Eqs. (22) and (23) as limiting cases of a Landau-type theory

$$P(m) \propto \exp\left[-\frac{8}{3}L^3\frac{f_L(m)}{k_B T}\right], \quad (24)$$

with an effective free energy density $f_L(m)$ [64]

$$f_L(m) = f_0 + \frac{1}{2L}rm^2 + \frac{1}{4}u_Lm^4 - Hm, \quad (25)$$

where we now have added the magnetic field. Moreover, Eq. (25) can be rewritten as

$$f_L(m) = f_0 + \frac{r}{4L}m_0^2 - \frac{r}{4Lm_0^2}(m - m_0)^2(m + m_0)^2 - Hm, \quad (26)$$

and thus Eq. (26) immediately leads to Eqs. (22) and (23) if $r = r_0 t, r_0$ being a constant. Since $m_0^2 = -r/(Lu_L)$, we recover a mean-field exponent $\beta = 1/2$ for the power law $m_0 = \hat{B}|t|^\beta$, as expected for a Landau type theory. Of course, such a mean-field relation for m_0 is consistent with the jump of the magnetization expected in the thermodynamic limit (Fig. 1) only if the critical amplitude \hat{B} diverges as L tends to infinity.

The considerations discussed so far do not give any clue where the basic nonlinearity responsible for deviations of $f_L(m)$ from Gaussian behavior comes from. Disturbingly, the t dependence of m_0 (supposedly valid for $m_0/m_b \ll 1$) is inconsistent with that which follows when one uses the expression $\ell_0 = \tilde{\ell}_0/|t|$ ($\tilde{\ell}_0$ being a critical amplitude) from Eq. (4) in Eq. (16). The approach of m_0/m_b to its saturation value unity

goes as $m_0/m_b - 1 \propto (L|t|)^{-3}$. Assuming that the term $u_L m^4$ describes physical effects due to the existence of corners, which take a fraction of $1/V \propto L^{-3}$ of the volume, a plausible assumption is [31] $u_L = u/L^3$ ($=u/L^d$ in d dimensions). As a consequence, one predicts

$$m_0 = L \sqrt{\frac{r_0}{u}} (-t)^{1/2}. \quad (27)$$

Of course, the condition $m_0/m_b \ll 1$ requires $L^2|t| \ll 1$. As we shall see below, in this regime all singular behavior is smeared out due to finite size rounding and, hence, Eq. (27) is not directly observable. The same problem occurs for the critical isotherm, which follows from Eq. (25) for $r=0$, $H \neq 0$,

$$\left(\frac{\partial f_L(m)}{\partial m} \right)_{t,H} = u_L m^3 - H = u(m/L)^3 - H = 0 \quad (28)$$

as

$$m_{0,t=0}(H) = L(H/u)^{1/\delta}, \quad \delta = 3, \quad (29)$$

i.e., the critical amplitude of the power law $m_0(H)|_{t=0} = \hat{D}H^{1/\delta}$ scales again proportional to L . If we generalize the problem to hyper-bipyramidal geometry in general dimensionality d , the result $\Gamma_{\pm} \propto L$ remains unchanged, while the other critical amplitudes become $\hat{B} \propto L^{(d-1)/2}$, $\hat{D} \propto L^{d/3}$ [31]. Finally we note that $f_L(m_0) = f_0 + r m^2 / (4L) = f_0 - L(r_0 t)^2 / (4u)$ for $t < 0$, as expected from Fig. 3. For $|t|$ of order $1/L^2$ the depression of $f_L(m)$ relative to f_0 is only of order L^{-3} , i.e., negligible on the scale of Fig. 3. Only for $|t| \sim 1/L$ a free energy of order $1/L$ is obtained.

The concept that the dominant statistical fluctuations are the “breather modes,” i.e., fluctuations of the uniform magnetization, fluctuations with a zero-dimensional phase space [21], is reminiscent of the behavior of Ising-like systems in high dimensionalities, $d > 4$, which exhibit mean-field critical behavior [65] but nevertheless for a description of finite size rounding these variations of the uniform magnetization need to be taken into account. In brief, the statistical mechanics of this latter problem is formulated [43–45] in terms of a partition function,

$$Z = \int dm \exp[-L^d f(m) / k_B T], \quad (30)$$

assuming a d -dimensional hypercubic lattice of linear dimension L with periodic boundary conditions, where (f_0 is a constant)

$$f(m) = f_0 + \frac{1}{2} r m^2 + \frac{1}{4} u m^4 - H m, \quad r = r' t, t = T/T_c - 1. \quad (31)$$

With the magnetization distribution,

$$P_L(m) = Z^{-1} \exp[-L^d f(m) / k_B T], \quad (32)$$

its moments are then calculated as

$$\langle m^k \rangle = \int m^k P_L(m) dm. \quad (33)$$

In this problem, however, u is a constant and does not depend on L , nor does any other L dependence appear in $f(m)$ as given in Eq. (31). With a little algebra [43–45] it is then straightforward to show that for $H=0$ the moments $\langle m^k \rangle$ (for k even, odd moments all vanish) scale as

$$\langle m^k \rangle = L^{-kd/4} \hat{M}_k(tL^{d/2}), \quad (34)$$

\hat{M}_k being scaling functions that can be explicitly derived from Eqs. (30)–(33).

Here we follow exactly the same procedure, the only difference being that Eq. (31) needs to be replaced by Eq. (25), with $u_L = u/L^3$. Thus we obtain, writing $\Psi = m/m_0$ and considering $H=0$ for simplicity,

$$P_L(\Psi) = \frac{\exp\left[-\frac{m_0^2 L^3}{3k_B T \chi'} (\Psi^2 - 1)^2\right]}{\int_{-\infty}^{+\infty} d\Psi \exp\left[-\frac{m_0^2 L^3}{3k_B T \chi'} (\Psi^2 - 1)^2\right]}. \quad (35)$$

It is seen that this distribution depends only on a single parameter, namely,

$$\frac{m_0^2 L^3}{k_B T \chi'} = L^2 \frac{r_0}{u} \frac{L^3}{L(2r_0 t)} = \frac{2}{u} (r_0 t L^2)^2, \quad (36)$$

and hence one finds that all moments are functions of this single parameter as well,

$$\langle |\Psi|^k \rangle = f_k(tL^2), \quad (37)$$

where the scaling function f_k is defined in terms of Eq. (35) by simple integrals. Since

$$\langle |m|^k \rangle = m_0^k \langle |\Psi|^k \rangle = \left(\frac{r_0 L^2 t}{u} \right)^{k/2} \langle |\Psi|^k \rangle \equiv \tilde{m}_k(tL^2), \quad (38)$$

also the scaling function \tilde{m}_k is a function of the scaling variable tL^2 again; there is no L -dependent prefactor, unlike Eq. (34).

It is useful to consider the behavior right at $t=0$ separately, since then (if also $H=0$) we have simply

$$P_L(m) = \frac{1}{Z} \exp\left[\frac{-2um^4}{3k_B T}\right], \quad (39)$$

since the L dependence of the volume $V=8L^3/3$ is canceled by the L dependence of u_L , $u_L = u/L^3$. From Eq. (39) it is then obvious that all moments $\langle |m|^k \rangle_{t=0} = \tilde{f}_k(0)$ are simple constants. If a magnetic field is included, we similarly conclude

$$\langle m^k \rangle = \tilde{m}_k(tL^2, HL^3) \quad (40)$$

and in particular one finds that the zero-field susceptibility at $t=0$ is finite and proportional to the volume, $\chi(t=0) \propto L^3$. At this point we return to one—so far not really justified—key assumption of the present treatment, namely $u_L = u/L^3$. Equally well one could argue that the basic non linearity, $u_L m^4$, of the effective free energy density is due to line tension effects rather than caused by the presence of pyramid or cone corners, and hence $u_L = u'/L^2$ would result. As a consequence, $m_0^2 = r_0 |t| L / u'$, and one would still predict a diverg-

ing amplitude of the order parameter, $m_0=L^{1/2}\sqrt{r_0/u'}|t|^{1/2}$, and a finite size scaling variable [Eq. (36)] $m_0^2L^3/(k_B T \chi') \propto (tL^{3/2})^2$ instead of $(tL^2)^2$. The free energy then would become $f_L(m)=f_0-(r_0t)^2/u'$, i.e., for $|t|L^{3/2}$ of order unity it still would be of order L^{-3} , as expected, since the regime of finite size rounding corresponds to total free energy differences in the system of order $k_B T$. However, considering the distribution $P_L(m)$ for $t=0$ we would obtain $P_L(m)=Z^{-1}\exp[-(2L^3/3k_B T)u_L m^4]=Z^{-1}\exp[-(2u'/3k_B T)Lm^4]$, implying that for $t=0$ the moments scale as $\langle |m|^k \rangle \propto L^{-k/4}$. As will be demonstrated in Sec. III, such a behavior clearly contradicts observation.

It is clear that the treatment presented so far is extremely simplified, and one needs to discuss various corrections. For the Landau theory of phase transitions in the bulk at high dimensionalities [Eqs. (30)–(34)] one knows that nonuniform order parameter fluctuations are the leading source of higher order correction terms to Eq. (34) [66]. In our problem, the analogous fluctuations to consider would be nonuniform fluctuations of the interface. These fluctuations are correlated in a volume ξ_{\perp}^d in d dimensions, and the motion of the interface back and forth in such a correlated volume would cause a magnetization fluctuation of the order of $m_b^2 \xi_{\perp}^d$. Hence we conclude that a contribution $\Delta\chi$ to the susceptibility results:

$$k_B T \Delta\chi = L^d (\langle m^2 \rangle - \langle |m| \rangle^2) \propto m_b^2 \xi_{\perp}^d \propto |t|^{-d/2}. \quad (41)$$

We note that in $d=3$ this divergence has a stronger power than the leading Curie-Weiss term, Eq. (20), but it has a critical amplitude which is of order unity rather than of order L . In the regime $|t|L^2 \gg 1$ the asymptotic behavior predicted by Eq. (20) should dominate, but for $|t|L^2$ of order unity this correction may be non-negligible. Denoting the leading result of Eq. (20) by χ_0 , we have in $d=3$

$$\begin{aligned} \chi &= \chi_0 + \Delta\chi \propto L|t|^{-1} + \text{const}|t|^{-3/2} \\ &= L|t|^{-1} [1 + \text{const}(|t|L^2)^{-1/2}]. \end{aligned} \quad (42)$$

Thus in the region of the finite size rounding of the transition, the nonuniform fluctuations yield corrections that are of the same order as the corrections that would result from the scaling function $\tilde{m}_k(tL^2)$ in Eq. (38). Hence one cannot expect that moments $\langle |m|^k \rangle$ calculated from Eq. (35) are quantitatively accurate, therefore, we have not bothered to work them out in full detail. This result must be expected, of course, because the result $\xi_{\perp} \propto |t|^{-1/2}$ means that for $|t|L^2$ of order unity ξ_{\perp} is of order L , the whole length scale of the Ising bipyramid.

It is also of interest to consider the generalization of Eq. (42) to arbitrary dimensionality d , which yields

$$\chi = \chi_0 + \Delta\chi = L|t|^{-1} [r_0 + \text{const}/L|t|^{(d/2-1)}]. \quad (43)$$

This result shows that for “hyper-bipyramids” in $d > 3$ $\Delta\chi$ indeed becomes a correction, smaller than the terms resulting from the scaling function in Eqs. (35)–(37). Conversely, for $d < 3$, the corrections in the finite size scaling limit $|t|L^{d-1}$ of order unity are proportional to $L^{d(3-d)/2}$ and hence larger than the leading term of order r_0 . This marginal role of $d=3$ may indicate possible logarithmic corrections to finite size scaling. For $d < 3$ we expect a nontrivial description of finite size

effects with non-mean-field exponents. Monte Carlo studies of the $d=2$ square geometry with competing edge fields [67] corroborate this conclusion.

In addition to the effects of nonuniform interfacial fluctuations, there exist also corrections due to walls, edges and corners that invalidate the simple relation between the interface height ℓ_0 and the magnetization, Eq. (16). For example, from the regime where in Fig. 2 a negatively oriented domain meets positive surface fields, we expect a correction $4\sqrt{2}(L^2 - \ell_0^2)(\Delta m_s/m_0)/(8L^3/3)$ to Eq. (16), so that

$$\frac{m}{m_b} = 1 - (\ell_0/L)^3 - (3/\sqrt{2}) \frac{\Delta m_s}{m_b} \left(\frac{1}{L} - \frac{\ell_0^2}{L^3} \right), \quad (44)$$

Δm_s being a surface magnetization difference (per unit surface area). Additional corrections (of order L^{-2}) may result from the edges where the triangular surfaces of the pyramid meet. Thus a phenomenological relation between $y=m/m_b$ and $x=\ell_0/L$ is

$$y = 1 - A_0 x - A_1 x^2 - A_2 x^3, \quad (45)$$

where A_0, A_1 , and A_2 are phenomenological constants.

When ℓ_0 is close to L , Eq. (44) can be simplified as

$$\frac{m}{m_b} = 3 \left(\frac{L - \ell_0}{L} - \sqrt{2} \frac{\Delta m_s}{m_b} \frac{L - \ell_0}{L^2} \right), \quad (46)$$

which implies that in the linear relation between $(\langle m \rangle - m)/m_b \approx 4(\ell_0 - \ell)/L$ used to justify Eq. (17) a correction term [of relative order $\sqrt{2}(\Delta m_s/m_b)/L$] enters, giving rise to the replacement of the factor $L^2|t|$ in Eq. (18) by a linear combination of terms $L^2|t|$ and $L|t|$, causing thus additional corrections to finite size scaling.

III. SIMULATION RESULTS

Qualitative evidence for the actual occurrence of the transition sketched in Fig. 1 is presented in Fig. 4, showing two snapshots of the Ising bipyramid in the two “phases” caused by different values of the surface field. Note that we use an Ising nearest neighbor Hamiltonian

$$\begin{aligned} \mathcal{H} = & -J \sum_{\langle i,j \rangle}^{\text{bulk}} S_i S_j - J_s \sum_{\langle i,j \rangle}^{\text{surfaces}} S_i S_j - H_s \sum_i^{\text{upper surfaces}} S_i \\ & + H_s \sum_i^{\text{lower surfaces}} S_i - H \sum_i^{\text{all spins}} S_i, \end{aligned} \quad (47)$$

where the exchange constant is weakened if both spins i, j are in a surface plane, $J_s = J/2$. One can see that for $J/k_B T = 0.45, H_s/J = 1.00$ the magnetization is still predominantly negative, as anticipated in the schematic drawing of Fig. 2 (left part). In the negative domain only small clusters of positively oriented spins occur, and vice versa. For $J/k_B T = 0.25$ and $H_s/J = 0.77$, however, there is no majority of either positive or negative spins, as far as one can tell this from viewing the pyramid surfaces.

A more quantitative characterization of the transition is provided by contour diagrams (Fig. 5). Figure 5 shows that the schematic view of an interface at a height ℓ_0 over the

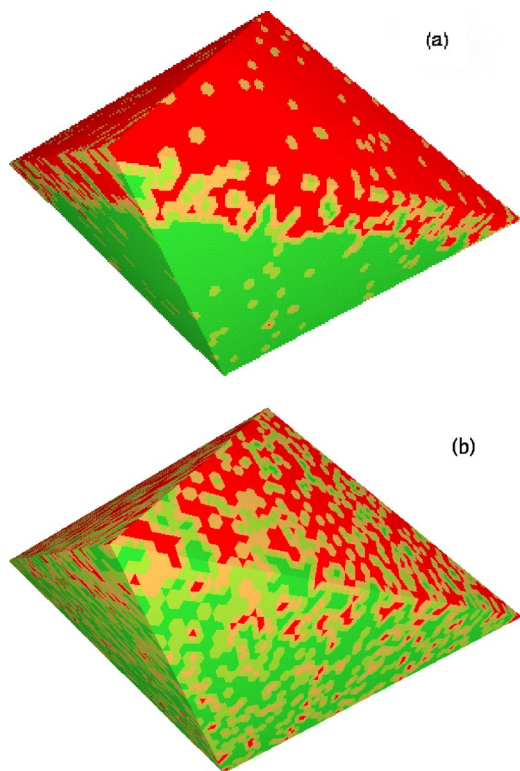


FIG. 4. (Color online) Snapshot pictures of the state of Ising bipyramids with $L=40$ and two surface fields: (a) $H_s/J=1.00, J/k_B T=0.45$, and (b) $H_s/J=0.77, J/k_B T=0.25$. The local magnetization m_i at the pyramid surfaces is coarse grained over each triangle of closest neighboring spins, thus taking on the values $m_i=-1, -1/3, 1/3, 1$ with i being the considered lattice site of the respective surface plane.

pyramid corner (Figs. 1 and 2) is a very crude oversimplification of reality: rather the interface is fairly broad, spread out over a thickness of many lattice spacings. Moreover, the interface is strongly bent and not at all horizontal. One can also see that the interface is not hitting the external surfaces, under a well-defined contact angle. Rather the midpoint contour $m(x, y, z)=0$ gradually bends over tangentially towards the external surfaces; see Fig. 5(a). Some crowding of contours near the external walls is always seen, implying that the corrections discussed in Eqs. (44)–(46) will make a substantial contribution [68]. Also in the symmetric situation [Fig. 5(b)], where the interface is flat and not bent, and the contour $m(x, y, z)=0$ does coincide with the basal plane, one can see that the effective width of the interface is quite broad. Due to this interfacial broadening, we expect that the details of the singular shape of the system (external surfaces with competing surface fields meet at $z=0$ under a sharp angle, $2\alpha=90^\circ$ here) do not matter, and if the bipyramid edges would be rounded away by a smoothly curved behavior, we should still observe the same behavior as in the present study as long as the radius of curvature in these smoothly curved regions is a finite constant, independent of L .

We next turn to a Monte Carlo test of the free energy constructions discussed in Fig. 3. For this purpose the surface free energy difference $f_s(H_s)$ is needed, and in order to

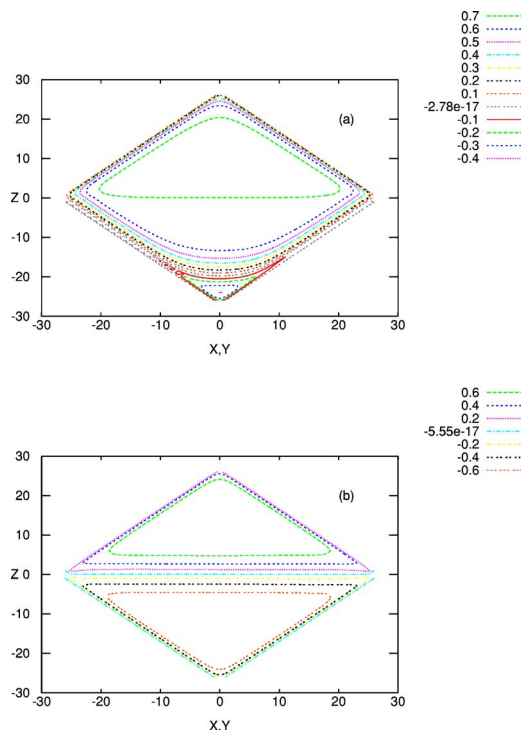


FIG. 5. (Color online) Contour plots presenting curves of constant magnetization (as shown in the key of each figure) as a function of position (z and x or y , respectively, choosing the coordinate origin in the center of mass of the bipyramid) for $L=26, k_B T/J=4, J_s/J=1/2$, and $H_s=0.6$ (a) and 0.8 (b).

find this quantity we apply thermodynamic integration methods [10,69], as done in our recent study of wedge filling [30].

Writing $f_{s+}(H_s), f_{s-}(H_s)$ for the surface excess free energies of the bulk phases with positive (+) and negative (−) magnetization and using the symmetry relation for the Ising model $f_{s-}(H_s)=f_{s+}(-H_s)$, we find that the required surface free energy difference can be written as $f_s(H_s)=f_{s+}(H_s)-f_{s+}(-H_s)$. Recalling the relation from surface thermodynamics of ferromagnets [70]

$$M_{s+}(H_s) = - \left(\frac{\partial f_s}{\partial H_s} \right), \quad (48)$$

where $M_{s+}(H_s)$ is the local magnetization per spin in the surface plane of an Ising ferromagnet with positive magnetization in the bulk, subject to surface field H_s , we recognize that the required free energy difference can be written as

$$f_s(H_s) = \int_{-H_s}^{H_s} M_{s+}(H'_s) dH'_s. \quad (49)$$

Figure 6(a) shows a plot of M_s versus H_s for the Ising bipyramids with various linear dimensions L as used in the present study. In principle, for an accurate estimation of $f_s(H_s)$, one should use not bipyramid surfaces but rather surfaces of large parallelepipeds (oriented with the same angle α relative to the plane $z=0$ as studied here), where effects due to edges and corners could be avoided by using suitably “staggered” periodic boundary conditions. Such a study has

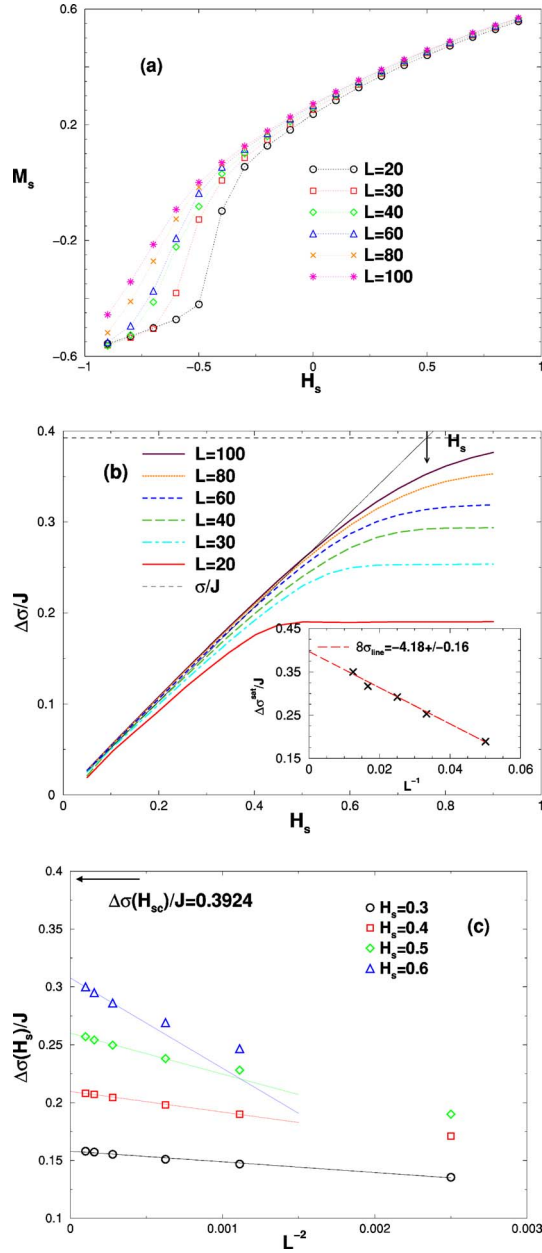


FIG. 6. (Color online) (a) Local magnetization per spin, M_s , in the surface plane [traditionally this quantity [70] is denoted as M_1 , to avoid confusion with the surface excess contribution m_s , to the total magnetization [cf. Eq. (44)], plotted versus the local surface magnetic field, using parameters $k_B T/J=4$, $J_s/J=1/2$, and linear dimensions L in the range $20 \leq L \leq 100$, as indicated. (b) Surface free energy difference $\Delta\sigma(H_s)/J$ plotted vs surface magnetic field H_s , as obtained from the data in part (a) via thermodynamic integration, Eq. (49). The full straight line shows the result of an extrapolation of $F_s(H)/J$ to the thermodynamic limit [see part (c)]. Broken horizontal straight line marks the value [71] of the interfacial tension, σ , of the Ising model at $k_B T/J=4$. The inset shows the extrapolation of the apparent plateau values (reached at $H_s=0.9$) of $\Delta\sigma/J$ versus L^{-1} . Arrow on top shows $H_{sc}=0.76$. (c) Finite size extrapolation of the surface free energy difference $\Delta\sigma(H_s)/J$ plotted vs L^{-2} , for four different choices of H_s , as indicated. Arrow shows the expected value of $\Delta\sigma(H_{sc})/J$ at the phase transition.

not been attempted here, rather we work with the bipyramid geometry throughout, but we then have to carefully consider the finite size effects, which are indeed quite pronounced [Figs. 6(b) and 6(c)]. Here $\Delta\sigma(H_s) = \sqrt{2}f_s(H_s)$, to account for the fact that the total surface area of the triangular facets of the pyramid is $\sqrt{2}(2L+1)^2$ in our model, while the total surface area of the basal plane is $(2L+1)^2$, measuring lengths in units of the lattice spacing. The corresponding value of the interface tension of a planar interface in the Ising model at $k_B T/J=4$, $\sigma/J=0.3924$ [71], is indicated by a dashed horizontal line. In principle, we expect that $\Delta\sigma/J$ near H_{sc} is a straight line, which intersects σ/J precisely at H_{sc} . In fact, the values of $\Delta\sigma(H_s)$ extrapolated to the thermodynamic limit do show such a behavior, yielding $H_{sc}=0.76$. However, for all finite L the curves $\Delta\sigma/J$ smoothly bend over, and reach horizontal plateaus for large H_s , which are substantially lower than σ/J . In terms of Fig. 6(b), the occurrence of these plateaus is understood from the fact that M_s for sufficiently negative H_s already obeys the symmetry $M_s(H_s) = -M_s(-H_s)$, because the sign of the magnetization in the corresponding pyramid has changed when the interface has moved towards the basal plane. For fields H_s where this symmetry holds the integral in Eq. (49) yields vanishing further contributions, resulting in a horizontal variation of $F_s(H_s)$ with H_s in this regime. Qualitatively, the behavior seen in Fig. 6(b) closely resembles the expected behavior as hypothetically sketched in Fig. 3. The linear extrapolation of the saturation plateaus $\Delta\sigma^{sat}/J$ versus L^{-1} [inset of Fig. 6(b)] is nicely consistent with this picture, since the linearity of the plot asserts that the depression of the plateaus indeed is a line tension effect, and the extrapolated value ($\Delta\sigma^{sat}/J \approx 0.39$) agrees with σ/J within the statistical error. From the slope of the broken straight line in the inset in Fig. 6(b) we deduce the estimate

$$8\sigma'_{line}/J = -4.18 \pm 0.16. \quad (50)$$

Unfortunately, we are not aware of any estimates of σ'_{line} for our geometry in the literature, to which our result could be compared.

In the regime where H_s is small, so that the bipyramid has essentially a uniform magnetization, apart from the region close to the lower pyramid corner [cf. Fig. 5(a)], the finite size correction to the surface free energy difference $\Delta\sigma(H_s)$ varies proportional to L^{-2} , as expected for a corner correction [Fig. 6(c)]. Unfortunately, a reliable extrapolation of $\Delta\sigma(H_s)$ in the region near H_{sc} would require one to simulate much larger systems than was possible for us.

We now turn to the description of the phase transition in terms of the moments $\langle |m|^k \rangle$ of the distribution function $P_L(m)$ of the magnetization (Fig. 7). Note that here and in the following m is the magnetization per spin and not normalized by m_b . A striking fact is the common intersection point of the $\langle |m| \rangle$ versus H_s curves (part a) for a broad range of choices for L , at $H_{sc}=0.76 \pm 0.005$. This value of the intersection point is fully in accord with the estimate resulting from the free energy intersections, obtained in Fig. 6(b). The inset illustrates the fact that the slope of the curves $\langle |m| \rangle$ vs H_s at $H_s=H_{sc}$ increases dramatically with L ; in fact, the data are

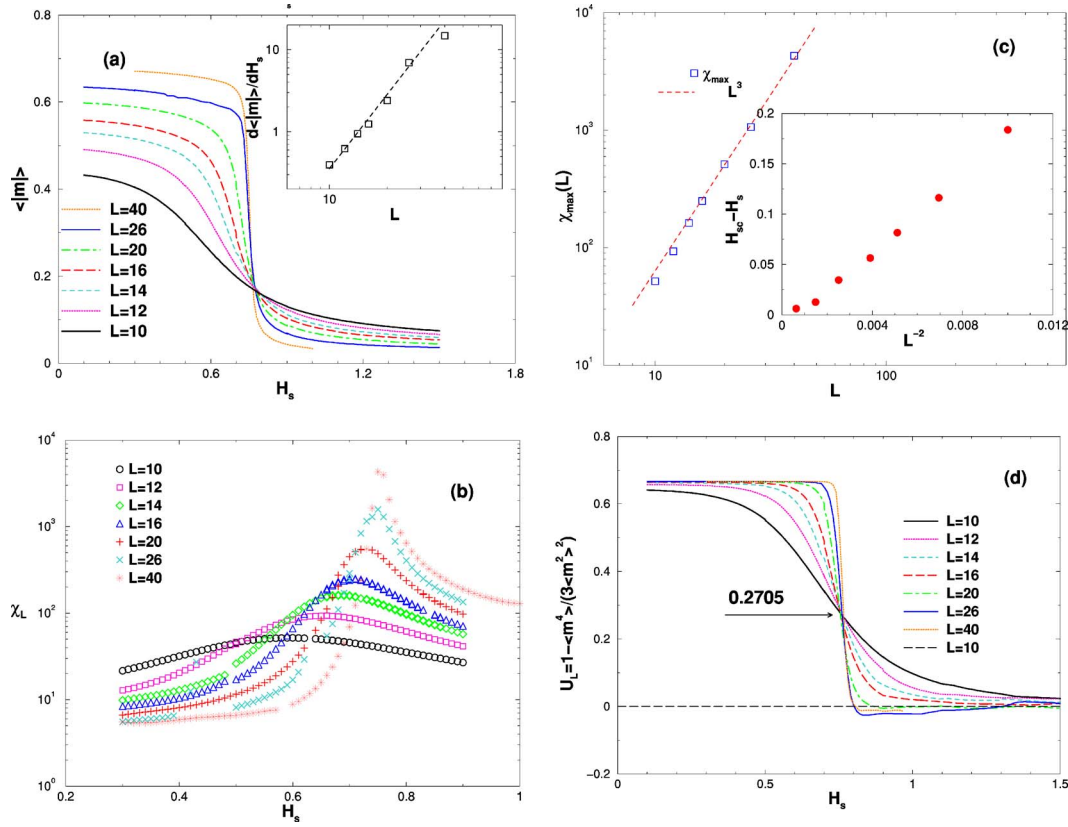


FIG. 7. (Color online) (a) Plot of the absolute value $\langle |m| \rangle$ of the magnetization of the Ising bipyramid versus the surface magnetic field H_s , for $k_B T/J=4.0, H=0, J_s/J=0.5$, and various linear dimensions L in the range $10 \leq L \leq 40$, as indicated. Inset shows a log-log plot of the slope at the common intersection point vs L . The straight line illustrates the theoretical value of the slope. (b) Plot of the susceptibility, calculated from magnetization fluctuations as $k_B T \chi_L = L^3(\langle m^2 \rangle - \langle |m| \rangle^2)$, as a function of the surface field H_s , including various linear dimensions L in the range $10 \leq L \leq 40$, as indicated. System parameters are the same as in part (a). Note the logarithmic scale of the ordinate. (c) Log-log plot of the susceptibility maximum, $\chi_{\max}(L)$, versus linear dimension, for the systems shown in part (b). Broken straight line illustrates the expected relation $\chi_{\max}(L) \propto L^3$. Inset shows the location of the maximum of χ_L, H_s^{\max} , plotted vs L^{-2} , to illustrate the convergence of H_s^{\max} towards H_{sc} as $L \rightarrow \infty$. (d) Cumulants U_L [Eq. (51)], plotted vs H_s , for various L as shown in the figure, for the same system parameters as used in parts (a) and (b).

roughly compatible with the behavior $(d\langle |m| \rangle/dH_s)_{H_{sc}} \propto L^2$, that one immediately derives from the scaling description, Eq. (38). Such a rapid increase of the slope $(d\langle |m| \rangle/dH_s)_{H_{sc}}$ is rather uncommon for normal second order transitions. From the curve for $L=40$ it is already easy to guess the limiting behavior, namely $\langle |m| \rangle = m_b \approx 0.75$ for $H_s < H_{sc}$, while $\langle |m| \rangle = 0$ for $H_s > H_{sc}$. Nevertheless, this jump of $\langle |m| \rangle$ resulting in the thermodynamic limit should not be mistaken for a standard first order transition—rather one deals here with the limiting case of a second order transition, where the critical amplitude diverges, and hence the critical region is exceedingly narrow. Figure 7 demonstrates that the susceptibility develops a sharp peak of rapidly increasing height, as L increases. As expected from the Curie-Weiss law with the divergent critical amplitude, the curves do not settle at a common L -independent function away from $H_s = H_{sc}$. But the data clearly indicate a gradual growth of χ_L with H_s as H_{sc} is approached from either side of the transition, and the width over which this peak is rounded rapidly shrinks as L is increased. There is not a convergence to a delta function singularity that would characterize a standard first order transition [40,41].

A direct analysis of these data, not requiring any bias from theory, examines the growth of the peak height with L , and the scaling of the peak position $H_s^{\max} - H_{sc}$ with L [Fig. 7(c)]. One nicely recognizes that these data are also compatible with a transition at $H_{sc} \approx 0.76$, and the relation $\chi_{\max}(L) \propto L^3$ implies that the maximum values of $\langle m^2 \rangle - \langle |m| \rangle^2$ are of order unity, as expected on the basis of Eq. (38). Unlike first order transitions (where also the susceptibility peak height increases proportional to the volume) the width of the susceptibility peak does not shrink to zero for $L \rightarrow \infty$.

A standard method to locate critical points for various phase transitions is to check for intersections of the reduced fourth order cumulant [41–43],

$$U_L = 1 - \langle m^4 \rangle / (3\langle m^2 \rangle^2). \quad (51)$$

Plotting hence U_L vs H_s for various L should yield a common intersection point at $H_s = H_{sc}$. Figure 7(d) shows that this simple recipe works here rather well again, confirming the previous estimate $H_{sc} \approx 0.76$. If one accepts Eq. (39) as a description of the distribution at H_{sc} , one predicts for the value of U^* of the cumulant at the intersection point the value $U^* = 1 - \Gamma(5/4)\Gamma(1/4)/[3\Gamma(3/4)^2] \approx 0.2705$. The arrow

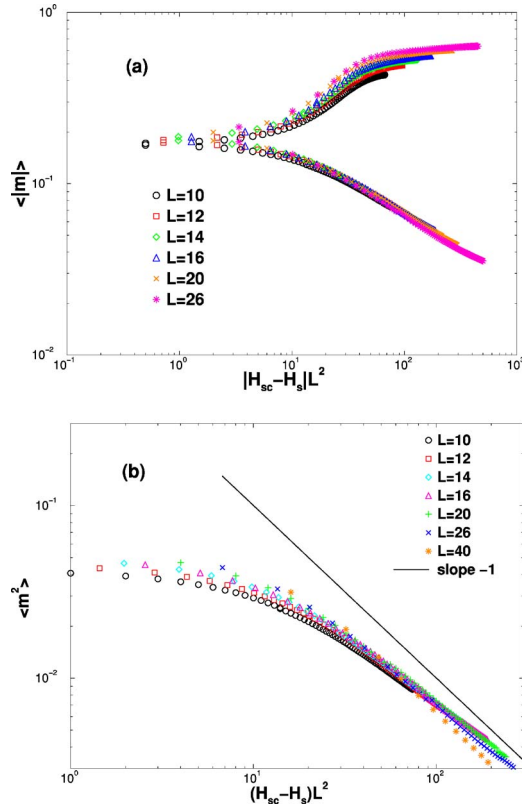


FIG. 8. (Color online) (a) Absolute value of the magnetization $\langle |m| \rangle$ plotted vs the scaling variable $|H_s - H_{sc}|L^2$, using the data of Fig. 7, and $H_{sc}=0.76$ and various L as indicated in the figure. (b) Plot of the second moment, $\langle m^2 \rangle$, vs the scaling variable $(H_s - H_{sc})L^2$, using $H_{sc}=0.76$ and including data only for $H_s > H_{sc}$. Various choices of L are shown as indicated. The straight line shows the slope of the asymptotic Curie Weiss law, $\langle m^2 \rangle \propto (tL^2)^{-1}$.

in Fig. 7(d) shows that this value is in very good agreement with the data. Interestingly, these data develop not only a common intersection point, but also a shallow minimum for $H_s > H_{sc}$. This is somewhat reminiscent of the behavior at thermally driven first order transitions, such as occur in the q -state Potts model in $d=3$ dimensions for $q \geq 3$, where U_L is known to exhibit a very deep minimum $U_L^{min} \propto -L^3$ [72]. So the behavior of the cumulant is again indicative of a second order transition that is close to a first order transition.

We now turn to a more detailed test of the finite size scaling predictions, in particular of Eq. (38). Figure 8 shows scaling plots of the magnetization and the magnetization square. Using $|H_{sc} - H_s|L^2$ as scaling variables in part (a), both branches of the scaling functions for $H_s < H_{sc}$ (upper branch) and $H_s > H_{sc}$ (lower branch) are combined in a single plot. However, the “data collapsing” on master curves in parts (a) and (b) is not really perfect, and some corrections to scaling are clearly seen. However, as pointed out above [see Eqs. (44)–(46) and the accompanying discussion], our scaling description has ignored contributions such as due to the surface excess magnetization m_s . Figure 9 shows a fit of data for the magnetization to Eq. (45) to test the size dependence, and thus it is shown that indeed important corrections are present [68].

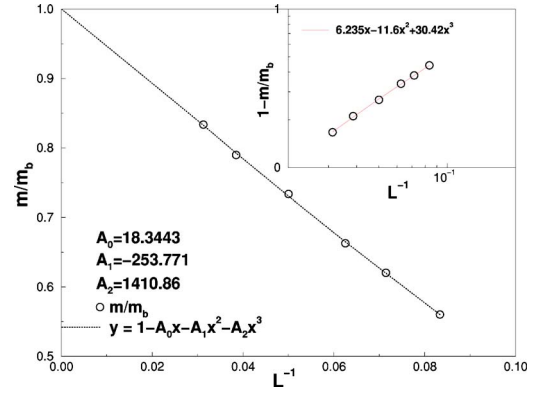


FIG. 9. (Color online) Position of the maximum of the distribution $P_L(m)$ at $H_s=0.73$ plotted vs L^{-1} , for the parameters $k_B T/J = 4.0$ and $J_s/J=1/2$. The bulk magnetization is $m_b=0.750$. The numerical data are fitted to Eq. (45), and the constants A_0, A_1, A_2 are quoted in the figure. Inset shows the difference $1 - m/m_b$ vs L^{-1} on a log-log plot.

The simulation data in Fig. 7 were extracted from an analysis of the probability distribution $P_L(m)$ of the magnetization, m , in the finite bipyramid, and since $P_L(m)$ plays a key role in our phenomenological description (Sec. II), we discuss $P_L(m)$ in detail now. Figure 10(a) shows that in the phase where the interface coincides with the basal plane of the bipyramid, $P_L(m)$ is perfectly described by the simple Gaussian, Eq. (21). From Fig. 7(d) we have already seen that the fourth order cumulant rapidly tends to zero for $H > H_{sc}$ as $L \rightarrow \infty$. The very good Gaussian fits of Fig. 7(a) imply that all higher order cumulants vanish as well. Of course, this behavior is plausible due to the rapid decrease of the fourth order term $u_L m^4/4$ in Eq. (25) as $L \rightarrow \infty$, since $u_L \propto L^{-3}$. Thus, for $(H_s - H_{sc})L^2 \gg 1$ the second moment $\langle m^2 \rangle$ shown in Fig. 8(b) already contains the full information on the distribution.

Figure 10(b) demonstrates now the smooth change of $P_L(m)$ from the single Gaussian to the double Gaussian when for fixed L the strength of the surface field is varied. This behavior is fully in accord with expectations for second order phase transitions. For a first order transition (e.g., a first order interface localization-delocalization transition has been recently studied both for an Ising system in thin film geometry with $J_s/J=1.5, H_s/J=0.25$ [73] and for models of confined polymer mixtures [59,74]) the corresponding distribution $P_L(m)$ near the transition has a pronounced three-peak structure: two peaks have nonzero positive or negative magnetization, and the third peak occurs for $m=0$ (e.g., see Fig. 7c of Ref. [73] for an explicit example). In contrast, here we expect near the transition a single very flat and broad peak [whose width should not shrink with increasing linear dimension L , as emphasized in Eq. (39)]. Figure 11 therefore examines the size dependence of $P_L(m)$ in the critical region, and part (a) shows that indeed one can find for each L a field $H'_s(L)$ such that $P_L(m)$ is essentially flat near $m=0$, and approximately the width of $P_L(m)$ stays independent of L when L increases, while $H'_s(L) \rightarrow H_{sc}=0.76$ as L increases.

Ideally, one might have expected that Eq. (39) should hold strictly for $H_s = H_{sc}$ (i.e., $t=0$). However, the small variation of $H'_s(L)$ with L that is implied by Fig. 11(a) does not in-

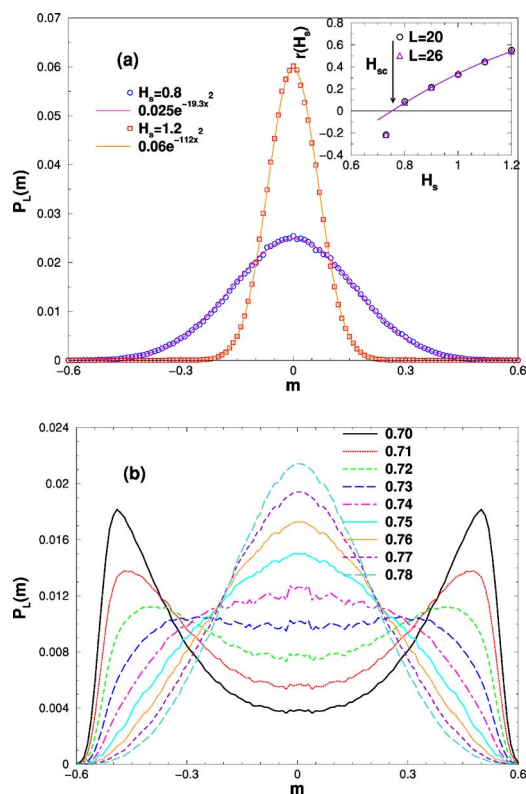


FIG. 10. (Color online) (a) Probability distribution of the magnetization $P_L(m)$ for fields $H_s > H_{sc}$, outside the critical region, using the parameters $L=20, k_B T/J=4, J_s/J=1/2$, and $H_s=0.8$ or 1.2 , respectively. Curves through the data points show fits to the simple Gaussian, as indicated in the figure. The inset shows the function $r(H_s)$, obtained from such fits (for $L=26$) to demonstrate the change of sign near H_{sc} . The data points for $H_s=0.73$ are taken from Fig. 11(b). (b) Probability distribution $P_L(m)$ of the magnetization, m , of an Ising bipyramid for $L=20, k_B T/J=4, J_s/J=0.5$, and $H=0$. Curves show various surface fields H_s/J , as indicated in the key.

validate our phenomenological theory of Sec. II at all: as is well known [38–43] for finite systems there is no unique “pseudocritical” point, due to the finite size rounding different criteria to locate a “pseudocritical” point for a finite system yield results differing from each other (and from the true location of the critical point) by amounts which are of the same order as the rounding, i.e., $t \propto L^{-2}$ in our case. Such an argument would imply $H'_{sc}(L) - H_{sc} \propto L^{-2}$ here. Unfortunately, our simulation data are not accurate enough to check this relation [and also a larger range of linear dimensions L than what is available for Fig. 11(a) would be desirable].

If a more rapid variation of $H'_{sc}(L) - H_{sc}$ than the second power of $1/L$ results, it could be attributed to corrections to finite size scaling, some of which were identified above [Eqs. (44)–(46)]. Despite all shortcomings that our numerical results still have, we consider Fig. 11(a) as a highlight of the present study, since it demonstrates that in the limit $L \rightarrow \infty$ at the transition point *macroscopic fluctuations* occur, the magnetization varies essentially everywhere in the region from $m = -0.5$ to $m = +0.5$ (in a situation where the bulk magnetization is $m_b \approx 0.75$), because the interface can correspondingly move freely up and down. Of course, viewing the

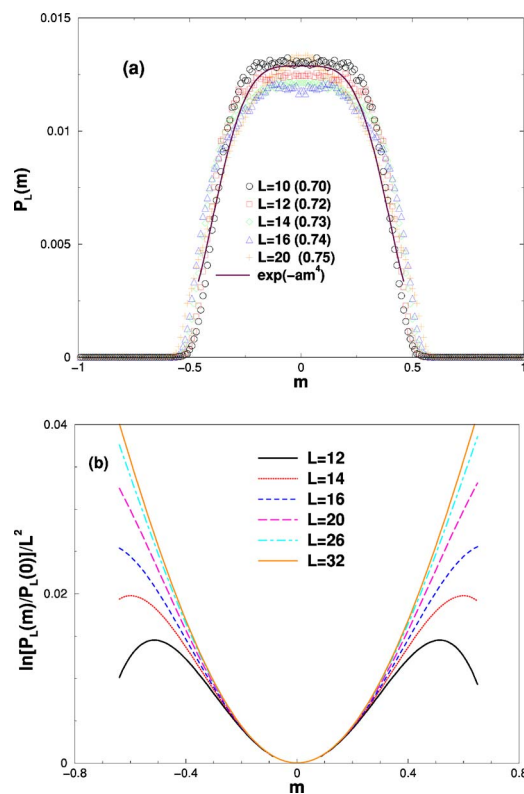


FIG. 11. (Color online) (a) Probability distribution $P_L(m)$, of the magnetization, m , of Ising bipyramids for $k_B T/J=4, J_s/J=0.5, H=0$, and various choices of L with accompanying choices of H_s/J for which a flat variation of $P_L(m)$ near $m=0$ was expected (these choices are quoted in the figure). Full curve shows the theoretical variation from Eq. (39), $P_L(m) \approx \exp[-am^4]$, with $a=2u/(3k_B T) = (1/3)u/J \approx 30.4$. (b) Plot of $\ln[P_L(m)/P_L(0)]/L^2$ vs m , for $k_B T/J=4, J_s/J=0.5, H=0$, at fixed $H_s/J=0.73$ and various L . The quadratic part near $m=0$ is described by $\ln[P_L(m)/P_L(0)]/L^2 = 0.11m^2$ independent of L .

Monte Carlo simulation as a stochastic process, such interface “motions” are extremely slow, and this “critical slowing down” [75] hampers severely the statistical accuracy of our Monte Carlo study, as expected [76,77]. Note that we have applied single spin flip Monte Carlo algorithms here, since the Swendsen-Wang algorithm [76,77] or related cluster algorithms are not offering any advantage in our case, working for temperatures distinctly below the bulk critical temperature T_{cb} and in the presence of nonzero surface fields.

Figure 11(b) shows then the magnetization distribution $P_L(m)$ for various L at a fixed value of H_s that is definitely below H_{sc} . One can see that with increasing values of L pronounced peaks develop with a very deep minimum in between; in fact, it was necessary to apply the so-called “multicanonical” sampling technique (see, e.g., Refs. [77,78]) in order to be able to sample more than 15 orders of magnitude in probability with sufficient accuracy.

We also remark that Fig. 11(b) is of a very different character than the corresponding distribution for a bulk Ising system for $T < T_{cb}$ [78]: there, also, a deep minimum in between the peaks corresponding to the two signs of the order parameter occurs, but it is very flat, almost horizontal, due to

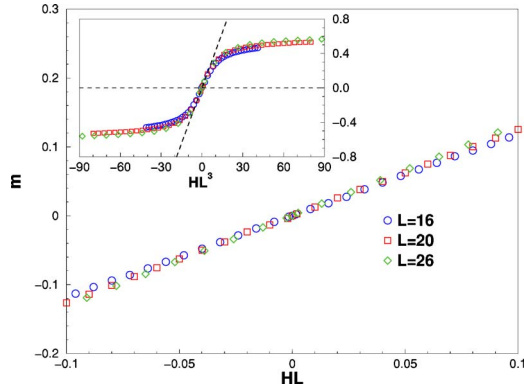


FIG. 12. (Color online) Plot of the average magnetization $\langle m \rangle$ as a function of the scaled field HL , for the parameters $k_B T/J = 4, J_s/J = 0.5, H_s = 1.2$, and three choices of L as indicated. Inset shows $\langle m \rangle$ vs HL^3 at $H_s = 0.76$.

configurations described as two phase coexistence (e.g., in a bulk Ising hypercube with periodic boundary conditions slab like domains occur). Here the minimum of $P_L(m)$ near $m = 0$ does not correspond to a “mixed state” of the degenerate phases (the interface being bound either to the top or to the bottom corner of the bipyramid, respectively), since no such “mixed state” can exist. Rather, the minimum corresponds to a uniform displacement of the interface from its stable position near one of the two corners to the basal plane.

Therefore the logarithm of the distribution $\ln P_L(m)$ near $m = 0$ is a simple parabola, as expected from Eqs. (24) and (25). This is demonstrated clearly because we have normalized $\ln P_L(m)$ such that all minima coincide. Dividing out the predicted L^2 dependence, we see that all curves near the minimum nicely superimpose. However, it is also clear from Fig. 11(b) that a fit to the form

$$\frac{\ln[P_L(m)/P_L(0)]}{8L^2/(3k_B T)} = -\frac{1}{2}rm^2 - \frac{u}{4L^2}m^4, \quad H = 0, \quad (52)$$

which would be implied by Eqs. (24) and (25), when $u_L = u/L^3$ is used, is not a good representation of the data for large m , and higher order terms (of order m^6, m^8, \dots) would be required. Of course, this is not surprising at all, since the saturation value of the magnetization at the considered temperature is $m_b = 0.75$, and the distribution spans the range from about $m \approx -0.6$ to about $+0.6$, i.e., close to the saturation values of m . Of course, Eq. (52) is supposed to be valid only for $|m| \ll m_b$. If we ignore this problem, the “best fit” values of the data in Fig. 11(b) would be $-4r/3k_B T = 0.11$, $2u/3k_B T = 30$. Nevertheless, it is reassuring that the estimates for r resulting from the fits in Figs. 10 and 11 [$8r/(3k_B T) = 0.56, 0.0965, -0.22$, for $H_s = 1.2, 0.8, 0.73$, respectively] yield a smooth curve $r(H_s)$, which has a zero close to $H_{sc} = 0.76$, though this curve is clearly not a simple straight line over the wide range of values for H_s that is considered here.

Now we turn, very briefly, to the behavior in nonzero bulk magnetic field H (Fig. 12). There are no surprises: we find that $\langle m \rangle$ is a function of a scaled field HL for $H_s > H_{sc}$, and of a scaled field HL^3 for $H_s = H_{sc}$, as expected from the

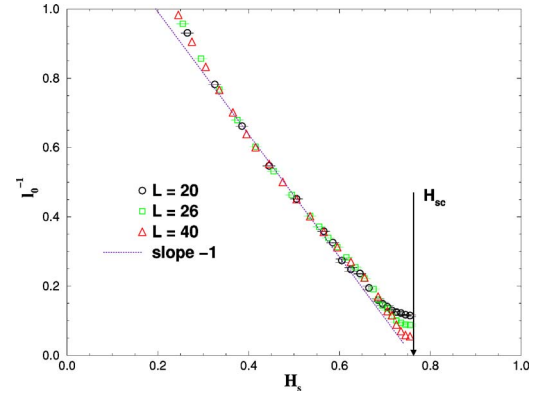


FIG. 13. (Color online) Plot of the inverse distance, ℓ_0^{-1} , of the interface from the bottom corner vs the surface magnetic field H_s . Here ℓ_0 is obtained from an analysis of the spatial magnetization distribution in the bipyramid (cf. Fig. 5). Three lattice sizes are shown, and the straight line marks the prediction $\ell_0^{-1} \propto H_{sc} - H_s$ according to Parry *et al.* [21].

theory of Sec. II [cf. Eqs. (20) and (40)]. If we include in Eq. (39) the magnetic field, $P_L(m) \propto \exp[-am^4 + 8L^3mH/3k_B T]$, we can readily calculate $m(H)$ at the critical point ($H_s = H_{sc}$, $t = 0$) as

$$m(H) = a^{-1/4} b [\Gamma(3/4)/\Gamma(1/4)] \{1 - (b^2/2)[1 - \Gamma(5/4)/(3\Gamma(3/4))] + \dots\},$$

where $b = 8a^{-1/4} L^3 H / (3k_B T)$. The resulting slope of $m(H)$ vs $L^3 H / J$, $m(H) \approx 0.043 L^3 H / J$ is again in good agreement with the numerical data in the inset of Fig. 12 and thus provides a test that the estimate of the constant a [$a \approx 30-34$, see Fig. 11(a)] is reasonable.

Finally, Fig. 13 considers the variation of the interface distance when the interface is close to a corner, and hence the theory of Parry *et al.* [21] should straightforwardly apply [i.e., Eq. (4) should hold]. Thus we plot simply ℓ_0^{-1} vs H_s to test the resulting linear variation. Indeed one recognizes that the data are nicely compatible with the predicted linear variation over a reasonable range of ℓ_0^{-1} , and the extrapolated intersection point with the abscissa agrees well with $H_{sc} = 0.76$. Of course, we cannot expect that this relation works for $\ell_0^{-1} \geq 1$, since the notion of an interface becomes absolutely meaningless when its distance from the pyramid corner becomes of the order of a single lattice unit, or even less. Conversely, finite size effects set in when $\ell_0 \approx L/2$. In view of the fact that the width of the critical distribution of the interface fluctuating around the basal plane of the bipyramid is of the order of $\Delta m \approx 0.5$, see Fig. 11(a), the strong finite size effect seen in Fig. 13 is not at all unexpected.

IV. DISCUSSION

We start by summarizing the main findings of this study.

(i) The Ising ferromagnet in a geometry with free surfaces, where surface fields are applied such that one half of the surface experiences a positive surface field and the other half experiences a negative surface field (of the same abso-

lute strength) has no total magnetization below the bulk critical temperature T_{cb} down to the filling transition temperature $T_f(H_s)$; see Fig. 1. This happens because the boundary conditions stabilize the interface, separating two domains of opposite orientation of the magnetization but taking equal volume. Below $T_f(H_s)$, the interface (in the limit $L \rightarrow \infty$) has essentially disappeared (it may be located at a finite distance of order unity close to either the top or the bottom corner if one specifically considers the bipyramid geometry as done in Fig. 1). Alternatively, this transition may be driven by variation of the strengths of the surface field H_s through its critical value $H_{sc}(T)$, note that $H_s = H_{sc}(T)$ simply is the inverse function of $T = T_f(H_s)$ in the (T, H_s) plane. This transition occurs in the way described here only if the parts of the surface where the surface field has the same sign are all adjacent to each other. For example for a bipyramid with boundary condition where the sign of the surface field alternates from one triangular surface to the adjacent one on the same pyramid, this condition would be violated, and no such phase transition occurs: rather one observes only a rounded phase transition near the bulk transition point [79].

(ii) As described in Fig. 3, in the thermodynamic limit the transition can be described in analogy with bulk first order transitions, where an intersection of the two branches of the free energy which describe the phases occurs. However, here, both branches are surface free energies, scaling like the surface area ($\propto L^2$) rather than the volume ($\propto L^3$). Although in the limit $L \rightarrow \infty$ the transition is characterized by a discontinuous jump in the magnetization [cf. Figs. 1 and 7(a)], it nevertheless is a second order transition, if the line tension of the boundaries of the interface where it meets the walls (Fig. 2, right part) is *negative*. This negative line tension makes it energetically favorable to stabilize already a domain of the minority phase for $H_s < H_{sc}$ with a mesoscopic linear dimension ℓ_0 , whereby ℓ_0 in the limit $L \rightarrow \infty$ diverges continuously, $\ell_0 \propto (H_{sc} - H_s)^{-1}$. Thus in a small interval of H_s close to H_{sc} in Fig. 7(a), or in a small interval of temperature near $T_f(H_s)$ in Fig. 1 (right part), the magnetization $\langle |m| \rangle$ of the system varies continuously from its saturation value m_b to zero. In the thermodynamic limit, however, the width of this interval shrinks to zero. On the other hand, this width over which the smooth variation occurs is of the same order as the width of the interval over which the finite size rounding of the transition occurs, namely of order L^{-2} . Therefore the power law, Eq. (27), predicted by a simple Landau-like theory that ignores finite size rounding, is nowhere clearly observable. In the finite size scaling plot [Fig. 8(a)] one cannot identify a branch with a slope 1/2 on the log-log plot on which the curves collapse. This is prevented by the saturation of the order parameter and, thus, the curves bend over to flat plateaus. This saturation is not described by the theory we have developed here, and it clearly violates the finite size scaling, as is evident from Fig. 8(a).

(iii) A particularly interesting behavior exhibits the total susceptibility of the system. Figures. 7(b) and 8(b) imply, in accord with our theory, that the susceptibility χ shows a Curie-Weiss-like divergence for $H_s > H_{sc}$, Eq. (20). The region of bulk fields, where this divergence is observable, shrinks to zero like $1/L$, because the critical amplitude in Eq.

(20) varies like L . There is a remarkable asymmetry between the behavior of the susceptibility in the regime $H_s > H_{sc}$ (where no total magnetization occurs) and the regime $H_s < H_{sc}$, however: in the latter regime, the total magnetization $\langle |m| \rangle$ essentially reaches its saturation value in the interval $H_{sc} - H_s \propto 1/L^2$, and this is the same regime over which the Curie-Weiss-like divergence of the susceptibility is rounded off. For $(H_{sc} - H_s)L^2 \gg 1$, however, $\langle |m| \rangle$ is almost identical to its saturation value, and the susceptibility converges towards the (small) susceptibility of a bulk Ising system, independent of size. The maximum value of the susceptibility scales like the system volume, L^3 , as in a first order transition [Fig. 7(c)], but unlike the latter the shape of the susceptibility maximum does not converge to a delta-function singularity [Fig. 7(b)].

(iv) A very special behavior is detected for the probability distribution of the order parameter (Figs. 10 and 11). On a scale of $|H_{sc} - H_s| \propto 1/L^2$ the shape of this distribution changes from a single Gaussian peak (for $H_s > H_{sc}$) to a double peak distribution (for $H_s < H_{sc}$), and the inverse width $r(H_s)$ vanishes linearly with H_s as H_{sc} is approached from above [see inset of Fig. 10(a)]. This transition from single to double peak shape happens via distribution $P_L(m) \propto \exp[-am^4]$, with a coefficient a that is *independent* of L [Fig. 11(a)]. This broadness of the distribution implies that in the limit $L \rightarrow \infty$ at $H_s = H_{sc}$ fluctuations of the magnetization occur which have a macroscopic, size-independent amplitude. The standard statement of statistical thermodynamics, that in the thermodynamic limit the relative magnitude of fluctuations ($|\Delta m|/m_b$) is negligibly small, is not at all true here. Again the behavior is completely different from a standard first-order transition: at the latter, the system would jump between $m=0$ and $m=-m_b$ and $+m_b$, whereas at the pathological second order transition found here the magnetization can fluctuate over a finite fraction of the interval between $-m_b$ and $+m_b$, characterized by the distribution of Fig. 11(a). At a first order transition, we would instead have three delta functions (at $m = \pm m_b$ and $m=0$, respectively) as an order parameter distribution. However, this particular behavior is easily accounted for by the Landau-type theory of Sec. II. In particular, for $H_s < H_{sc}$, the simulations confirm the behavior $\ln P_L \propto L^{-2}m^2$ near the minimum at $m=0$ [Fig. 11(b)].

(v) In the regime for $H_s < H_{sc}$, when the system is large enough so that $|m|$ is close to its saturation value m_b , the variation of the interface distance ℓ_0 counted from one of the corners is found to go as $\ell_0 \propto (H_{sc} - H_s)^{-1}$, as predicted by Parry *et al.* [21]. When ℓ_0 becomes comparable to $L/2$, this divergence is rounded off, as expected from the behavior of $P_L(m)$, since then a crossover from the theory of Ref. [21] to the behavior described by our Landau-like theory occurs. However, the detailed behavior in this crossover region is not yet fully understood.

(vi) We now discuss the extent to which similar behavior can be expected to be found for real systems, such as the liquid-gas transition in a suitable cavity, where half of the surface area has an energetic preference for the liquid (such that “incomplete wetting” of the liquid at the wall occurs) and the other half prefers the gas (i.e., an “incomplete dry-

ing” boundary condition). In this case one neither has a precise symmetry between liquid and gas in the bulk, nor can one expect a precise antisymmetry between the interactions at the two types of walls. Therefore the phase transitions will be shifted somewhat away from the chemical potential value at which phase coexistence can occur in the bulk. A similar smooth interpolation between “capillary condensation”-like behavior and “interface localization-delocalization” transitions has also been found for a model of a polymer blend in a thin film geometry confined between parallel plates at which surface fields act which do not have a particular symmetry [80]. It is encouraging that wetting phenomena in systems where chemically distinct substrates meet find increasing theoretical [25] and experimental attention [81]. An important constraint though is that for the fluids one has to consider the grand-canonical ensemble where the fluid in the cavity can exchange particles with a reservoir, and similarly for the binary fluid in the cavity also exchanges $A \rightleftharpoons B$ or vice versa must be possible, due to a connection with a suitable reservoir. If one considers a fluid in a cavity with a fixed

total number of fluid particles, or a binary mixture in a cavity with fixed relative concentration, this transition of Fig. 1 is completely suppressed: this situation would correspond to an Ising system at constant total magnetization, and hence by construction fluctuations of the uniform magnetization then are impossible. In Fig. 1 then the configuration with an interface present in the basal plane of the bipyramid is enforced at all temperatures. An interesting aspect is also the crossover between the transition studied here and the standard critical behavior near the bulk critical temperature (a crossover from wetting to critical adsorption [82]).

ACKNOWLEDGMENTS

This work has greatly benefitted from stimulating discussions with Andrew O. Parry, Amnon Aharony, and Siegfried Dietrich. One of us (A.M.) is grateful to the Deutsche Forschungsgemeinschaft for support under Grant No. 436 BUL 113/130.

-
- [1] W. T. Thompson (Lord Kelvin), *Philos. Mag.* **42**, 448 (1871).
 [2] S. J. Gregg and K. S. W. Sing, *Adsorption, Surface Area, and Porosity* (Academic, New York, 1982).
 [3] R. Evans, *J. Phys.: Condens. Matter* **2**, 8989 (1990).
 [4] L. D. Gelb, K. E. Gubbins, R. Radhakrishnan, and M. Sliwiska-Bartkowiak, *Rep. Prog. Phys.* **62**, 1573 (1999).
 [5] K. Binder, D. P. Landau, and M. Müller, *J. Stat. Phys.* **110**, 1411 (2003).
 [6] M. E. Fisher and H. Nakanishi, *J. Chem. Phys.* **75**, 5857 (1981); H. Nakanishi and M. E. Fisher, *J. Chem. Phys.* **78**, 3279 (1983).
 [7] R. Evans and P. Tarazona, *Phys. Rev. Lett.* **52**, 557 (1984).
 [8] D. Nicolaidis and R. Evans, *Phys. Rev. B* **39**, 9336 (1989).
 [9] K. Binder and D. P. Landau, *J. Chem. Phys.* **96**, 1444 (1992).
 [10] M. Müller and K. Binder, *Macromolecules* **31**, 8323 (1998).
 [11] O. Dillmann, W. Janke, M. Müller, and K. Binder, *J. Chem. Phys.* **114**, 5853 (2001).
 [12] P. Concus and R. Finn, *Proc. Natl. Acad. Sci. U.S.A.* **63**, 292 (1969).
 [13] R. Finn, *Equilibrium Capillary Surfaces* (Springer, Berlin, 1986).
 [14] Y. Pomeau, *J. Colloid Interface Sci.* **113**, 5 (1986).
 [15] E. H. Hauge, *Phys. Rev. A* **46**, 4994 (1992).
 [16] K. Rejmer, S. Dietrich, and M. Napiorkowski, *Phys. Rev. E* **60**, 4027 (1999).
 [17] A. O. Parry, C. Rascón, and A. J. Wood, *Phys. Rev. Lett.* **83**, 5535 (1999).
 [18] C. Rascón and A. O. Parry, *J. Chem. Phys.* **112**, 5157 (2000).
 [19] A. O. Parry, C. Rascón, and A. J. Wood, *Phys. Rev. Lett.* **85**, 345 (2000).
 [20] A. O. Parry, A. J. Wood, and C. Rascón, *J. Phys.: Condens. Matter* **12**, 7671 (2000).
 [21] A. O. Parry, A. J. Wood, and C. Rascón, *J. Phys.: Condens. Matter* **13**, 4591 (2001).
 [22] A. O. Parry, A. J. Wood, E. Carlon, and A. Drzewinski, *Phys. Rev. Lett.* **87**, 196103 (2001).
 [23] A. Bednorz and M. Napiorkowski, *J. Phys. A* **33**, L353 (2001).
 [24] A. O. Parry, M. J. Greenall, and A. J. Wood, *J. Phys.: Condens. Matter* **14**, 1169 (2002).
 [25] P. Jakubczyk and M. Napiorkowski, *Phys. Rev. E* **66**, 041107 (2002).
 [26] D. B. Abraham, A. O. Parry and A. J. Wood, *Europhys. Lett.* **60**, 106 (2002).
 [27] D. B. Abraham and A. Maciolek, *Phys. Rev. Lett.* **89**, 286101 (2002).
 [28] D. B. Abraham, V. Mustonen and A. J. Wood, *Europhys. Lett.* **63**, 408 (2003).
 [29] A. Milchev, M. Müller, K. Binder and D. P. Landau, *Phys. Rev. Lett.* **90**, 136101 (2003).
 [30] A. Milchev, M. Müller, K. Binder and D. P. Landau, *Phys. Rev. E* **68**, 031601 (2003).
 [31] A preliminary brief account of some of our results was given in A. Milchev, M. Müller, and K. Binder, *Europhys. Lett.* **70**, 348 (2005).
 [32] J. W. Gibbs, *The Collected Works of J. Willard Gibbs* (Yale University Press, London, 1957), p. 288.
 [33] J. S. Rowlinson and B. Widom, *Molecular Theory of Capillarity* (Clarendon, Oxford, 1982).
 [34] P. G. deGennes, *Rev. Mod. Phys.* **57**, 827 (1985).
 [35] J. O. Indekeu, *Int. J. Mod. Phys. B* **138**, 309 (1994).
 [36] J. Drelich, *Colloids Surf., A* **116**, 43 (1996).
 [37] T. Getta and S. Dietrich, *Phys. Rev. E* **57**, 655 (1998); W. Koch, S. Dietrich and M. Napiorkowski, *Phys. Rev. E* **51**, 3300 (1995); C. Bauer and S. Dietrich, *Eur. Phys. J. B* **10**, 767(1999).
 [38] M. E. Fisher, in *Critical Phenomena*, Proceedings of the 1970 Enrico Fermi International School of Physics, edited by M. S. Green (Academic, London, 1976), p. 1.
 [39] M. N. Barber, in *Phase Transitions and Critical Phenomena*, edited by C. Domb and J. L. Lebowitz (Academic, New York,

- 1983), Vol. 8, p. 145.
- [40] *Finite Size Scaling and the Numerical Simulation of Statistical Systems*, edited by V. Privman (Singapore, World Scientific, 1990).
- [41] K. Binder, in *Computational Methods in Field Theory*, edited by H. Gausterer and C. B. Lang (Springer, Berlin, 1992), p. 59.
- [42] K. Binder, *Z. Phys. B: Condens. Matter* **43**, 119 (1981).
- [43] K. Binder, *Z. Phys. B: Condens. Matter* **61**, 13 (1985).
- [44] E. Brézin and J. Zinn-Justin, *Nucl. Phys. B: Field Theory Stat. Syst.* **257** [FS14], 867 (1985).
- [45] E. Luijten, H. W. J. Blöte, and K. Binder, *Eur. Phys. J. B* **9**, 189 (1999).
- [46] J. Zinn-Justin, *Phys. Rep.* **344**, 159 (2001).
- [47] K. Binder and E. Luijten, *Phys. Rep.* **344**, 179 (2001).
- [48] F.-P. Buff, A. R. Lovett, and F. H. Stillinger, *Phys. Rev. Lett.* **15**, 621 (1965).
- [49] J. D. Weeks, *J. Chem. Phys.* **67**, 3106 (1977).
- [50] J. D. Weeks, *Phys. Rev. Lett.* **52**, 2160 (1984).
- [51] D. Jasnow, *Rep. Prog. Phys.* **47**, 1059 (1984).
- [52] V. Privman, *Int. J. Mod. Phys. C* **3**, 857 (1992).
- [53] K. Binder and M. Müller, *Int. J. Mod. Phys. C* **11**, 1093 (2000).
- [54] A. O. Parry and R. Evans, *Phys. Rev. Lett.* **64**, 439 (1990).
- [55] A. O. Parry and R. Evans, *Physica A* **181**, 250 (1992).
- [56] K. Binder, D. P. Landau, and A. M. Ferrenberg, *Phys. Rev. Lett.* **74**, 298 (1995).
- [57] K. Binder, D. P. Landau, and A. M. Ferrenberg, *Phys. Rev. E* **51**, 2823 (1995).
- [58] K. Binder, R. Evans, D. P. Landau, and A. M. Ferrenberg, *Phys. Rev. E* **53**, 5023 (1996).
- [59] M. Müller and K. Binder, *Phys. Rev. E* **63**, 021602 (2001).
- [60] A. Werner, F. Schmid, M. Müller, and K. Binder, *J. Chem. Phys.* **107**, 8175 (1997).
- [61] T. Kerle, J. Klein, and K. Binder, *Phys. Rev. Lett.* **77**, 1318 (1996).
- [62] L. D. Landau and E. M. Lifshitz, *Statistical Physics*, 3rd ed. (Pergamon, Oxford, 1980).
- [63] V. Privman, A. Aharony and P. C. Hohenberg, in *Phase Transitions and Critical Phenomena, Vol. 14*, edited by C. Domb and J. L. Lebowitz (Academic Press, London, 1991), p. 1.
- [64] Note that in Ref. [31] the factor $8/(3k_B T)$ was absorbed in the definition of $f_L(m)$.
- [65] M. E. Fisher, *Rev. Mod. Phys.* **46**, 587 (1984).
- [66] X. S. Chen and V. Dohm, *Int. J. Mod. Phys. C* **9**, 1105 (1998).
- [67] E. V. Albano, A. DeVirgiliis, M. Müller, and K. Binder, *J. Phys.: Condens. Matter* **15**, 333 (2003).
- [68] The authors are greatly indebted to Professor A. Aharony for a helpful discussion of this issue.
- [69] M. Müller and L. G. MacDowell, *Macromolecules* **33**, 3902 (2000).
- [70] K. Binder, in *Phase Transitions and Critical Phenomena, Vol. 8*, edited by C. Domb and J. L. Lebowitz (Academic Press, London, 1983), p. 1.
- [71] M. Hasenbusch and K. Pinn, *Physica A* **203**, 189 (1994).
- [72] K. Vollmayr, J. D. Reger, M. Scheucher, and K. Binder, *Z. Phys. B: Condens. Matter* **91**, 113 (1993).
- [73] B. J. Schulz, K. Binder, and M. Müller, *Phys. Rev. E* **71**, 046705 (2005).
- [74] M. Müller and K. Binder, *J. Phys.: Condens. Matter* **17**, S333 (2005).
- [75] P. C. Hohenberg and B. I. Halperin, *Rev. Mod. Phys.* **49**, 435 (1977).
- [76] K. Binder and D. W. Heermann, *Monte Carlo Simulation in Statistical Physics. An Introduction*, 4th ed. (Springer, Berlin, 2002).
- [77] D. P. Landau and K. Binder, *A Guide to Monte Carlo Simulations in Statistical Physics*, 2nd ed. (Cambridge University Press, Cambridge, UK, 2005).
- [78] B. A. Berg, U. Hansmann, and T. Neuhaus, *Phys. Rev. B* **47**, 497 (1993).
- [79] A. Milchev, A. De Virgiliis, and K. Binder (in preparation).
- [80] M. Müller, K. Binder, and E. V. Albano, *Europhys. Lett.* **50**, 724 (2000).
- [81] M. Geoghegan, C. Wang, N. Rehse, R. Magerle, and G. Krausch, *J. Phys.: Condens. Matter* **17**, S389 (2005).
- [82] A. Hanke, M. Krech, F. Schlesener, and S. Dietrich, *Phys. Rev. E* **60** 5163 (1999); G. Palagyi and S. Dietrich, *Phys. Rev. E* **70**, 046114 (2004).